NANOFLUID FLOW BETWEEN PARALLEL PLATES AND HEAT TRANSFER IN PRESENCE OF CHEMICAL REACTION AND POROUS MATRIX

S. JENA†, S.R. MISHRA‡, P. K.PATTNAIK§ and RAM PRAKASH SHARMA*

† *Department of Mathematics, Centurion University of Technology and Management, Odisha, India.*
‡ *Department of Mathematics, Siksha 'O' Anusandhan Deemed to be University, Bhubaneswar-751030, Odisha, India*
§ *Faculty, Department of Mathematics, College of Engineering and Technology, Odisha, India*
** Department of Mechanical Engineering, National Institute of Technology, Yupia, Papum Pare District, Arunachal Pradesh, Pin-791112, India. Corresponding Author Email: rpsharma@nitap.ac.in*

***Abstract*— This paper deals with nanofluid flow between parallel plates and heat transfer through porous media with a heat source /sink. The governing equations are transformed into self-similar ordinary differential equations by adopting similarity transformations and then the converted equations are solved numerically by Runge-Kutta fourth-order method. Special emphasis has been given to the parameters of physical interest which include Prandtl number, magnetic parameter, porous matrix, chemical reaction parameter, and heat source parameter. The results obtained for velocity, temperature, and concentration are shown in graphs. The comparison of the special case of this present result with the existing numerical solutions in the literature shows excellent agreement.**

***Keywords*— Parallel stretching plates, nanofluid, porous medium, MHD flow, chemical reaction, heat transfer.**

MOMENCLATURE

C nanofluid concentration (particles/mL)
C_p Specific heat (J K^{-1})
C_f skin friction coefficient
M Magnetic parameter (tesla)
h Distance between plates (m)
K_c Chemical reaction parameter (M / s)
k Thermal conductivity (W/(m·K))
K_p Permeability of the porous medium (m^2)
P_r Prandtl number
S_c Schmidt number
R Velocity parameter (m/s)
Nb Brownian motion parameter
T Fluid temperature (K)
Nt Thermophoretic parameter
u, v velocity components

Greek symbols

α Thermal diffusivity (m^2/s)
λ Suction parameter
η Similarity variable
μ Dynamic viscosity (Pa.s)
υ Kinematic fluid viscosity (m^2/s)
ρ Fluid density (kg/m^3)
σ electrical conductivity (S/m)

I. INTRODUCTION

The nanofluid has a wide range of applications in engineering and several technological purposes. This type of flow will frequently appear in many industrial and engineering processes and in those cases, the qualities of the final products depend to a great extent on the rate of cooling. So, to get the better product the heat transfer should be controlled. Such a system is used in a wide variety of manufacturing processes such as crystal growing, plastic extrusion, continuous casting, etc. The concept of nanofluid was introduced by Choi (1995) where he proposed the suspension of nanoparticles in a base fluid such as water, oil, and ethylene glycol. Nadeem *et al.* (2013) have studied about Oldroyd- B nanofluid. They have investigated 2-D boundary layer flow with heat transfer in a steady incompressible fluid where the sheet is stretched. Gangadhar *et al.* (2018a,b) made use of spectral relaxation numerical methods to tackle the problem of unsteady nanofluid flow over a stretching sheet (unsteady). They also considered the problem of heat and mass transfer in MHD mixed convection flow with chemical reaction and a magnetic field for a stretching surface. Bhukta *et al.* (2014) investigated the effects of heat and mass transfer on MHD viscoelastic fluid flow over a shrinking sheet embedded in a porous medium. Further, Baag *et al.* (2017) carried out a numerical study on the problem of MHD micropolar fluid over a vertical surface with a heat source and chemical reaction. Kar *et al.* (2013) extended the problem to three-dimensional free convective MHD flow over a vertical surface in a porous medium with a heat source and chemical reaction. Bhattacharyya *et al.* (2013) studied analytically the effects of MHD boundary layer Casson fluid flow with wall mass transfer over a stretching/shrinking sheet (permeable). Again an immediate investigation has been made by Nadeem *et al.* (2012). They have examined Casson fluid flow over an exponentially shrinking sheet (permeable). It is also about the MHD boundary layer flow. Gireesha *et al.* (2017) have extended their work by considering three-dimensional MHD Casson nanofluid flow with buoyancy effects over a stretching sheet with radiative heat transfer. By using a numerical method, Sharma *et al.* (2017a) solved the effects of heat source on hydromagnetic slip flow over a stretching sheet. Makinde *et al.*

(2017) extended the work to that of chemically reacting stagnation point slip flow towards a stretching sheet with thermal radiation. Sharma *et al.* (2017b) analyzed the radiation effects of non-Newtonian fluids flow over a variable thickness stretching sheet. Mahanthesh *et al.* (2018) have analyzed a three-dimensional steady flow of an incompressible conducting viscous fluid impinging on a stretching surface with thermal radiation. Makinde *et al.* (2016 a,b), and Khan *et al.* (2016) have studied the influence of magnetic field and convective heating on the boundary layer flow of a radiating nanofluid over a stretching surface embedded in a porous medium. Ibrahim and Makinde (2016) discussed the combined effects of convective boundary conditions and the magnetic field on the thermal stagnation point flow of Casson nanofluid past a stretching sheet. In this paper, he has discussed that the thermal boundary layer is formed when there is a temperature difference between the free stream fluid and solid-fluid interface. If the ambient fluid temperature is less than the temperature of the interface, then the kinetic energy increases between molecules of the adjacent fluid particles. Then the particles exchange the acquired kinetic energy with the adjacent layers and further go away from the interface. This process goes on so that and temperature gradients develop in the fluid. Lai and Kulacki (1990) have considered Newtonian fluid. They have discussed the heat transfer effect along a vertical surface considering along a vertical surface. Vajravelu *et al.* (2017) and Prasad *et al.* (2017, 2019) have shown their interest in the study of different aspects of nanofluid flow.

The present paper aims to discuss the analytic solution for nanofluid flow between parallel plates and heat transfer in the presence of chemical reaction and porous matrix. The method employed for the analytic solution of the nonlinear problem is Runge-Kutta fourth-order method.

II. MATHEMATICAL ANALYSIS

Steady two-dimensional, electrically conducting nanofluid flow between two parallel plates placed horizontally is considered. Both the plates are at a distance h apart embedding with a porous material. The flow is along the x-axis and y-axis is normal to it. Both the fluid and the plates rotate with an angular velocity. A uniform magnetic field of strength B_0 is applied in the direction normal to the plate and the system is rotating along y-axis. With these the boundary layer equations and corresponding boundary conditions are:

$$\frac{\partial u}{\partial x}+\frac{\partial v}{\partial y}=0 \tag{1}$$

$$\rho_f\left(u\frac{\partial u}{\partial x}+v\frac{\partial u}{\partial y}\right)=-\frac{\partial p^*}{\partial x}+\mu\left(\frac{\partial^2 u}{\partial x^2}+\frac{\partial^2 u}{\partial y^2}\right)-\sigma B_0^2 u-\frac{\nu u}{K_p'} \tag{2}$$

$$\rho_f\left(u\frac{\partial v}{\partial x}+v\frac{\partial v}{\partial y}\right)=-\frac{\partial p^*}{\partial y}+\mu\left(\frac{\partial^2 v}{\partial x^2}+\frac{\partial^2 v}{\partial y^2}\right) \tag{3}$$

$$u\frac{\partial T}{\partial x}+v\frac{\partial T}{\partial y}=\alpha\left(\frac{\partial^2 T}{\partial x^2}+\frac{\partial^2 T}{\partial y^2}\right)+\frac{(\rho c_p)_p}{(\rho c_p)_f}\times\left(D_B\left(\frac{\partial C}{\partial x}\frac{\partial T}{\partial x}+\frac{\partial C}{\partial y}\frac{\partial T}{\partial y}\right)+\frac{D_T}{T_C}\left(\left(\frac{\partial T}{\partial x}\right)^2+\left(\frac{\partial T}{\partial y}\right)^2\right)\right)+\frac{Q}{\rho C_p}(T-T_\infty) \tag{4}$$

$$u\frac{\partial C}{\partial x}+v\frac{\partial C}{\partial y}=D_B\left(\frac{\partial^2 C}{\partial x^2}+\frac{\partial^2 C}{\partial y^2}\right)+\frac{D_T}{T_0}\left(\frac{\partial^2 T}{\partial x^2}+\frac{\partial^2 T}{\partial y^2}\right)-K_c(C-C_h) \tag{5}$$

$$\left.\begin{array}{l} u=ax, v=0, T=T_h, C=C_h \text{ at } y=0 \\ u=0, v=0, T=T_0, C=C_0 \text{ at } y=h \end{array}\right\} \tag{6}$$

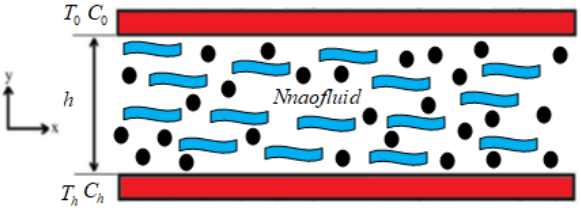

Fig. 1. Geometrical configuration

We now introduce the following dimensionless quantities:

$$\theta(\eta)=\frac{T-T_h}{T_0-T_h}, \phi(\eta)=\frac{C-C_h}{C_0-C_h} \tag{7}$$

Using the dimensionless quantities, the governing Eqs. (2)– (5) and boundary conditions (6) are as follows (see Seikholeslami *et al*., 2016):

$$f^{iv}+R(f'f''-ff''')-\left(M+\frac{1}{Kp}\right)f''=0$$

$$\theta''+R\mathrm{Pr}f\theta'+Nb\theta'\phi'+Nt\theta'^2+\lambda Pr\theta=0$$

$$\phi''+RScf\phi'+\frac{Nt}{Nb}\theta''-RScKc\phi=0 \tag{8}$$

$$\left.\begin{array}{l} f(\eta)=0, f'(\eta)=1, \theta(\eta)=1, \phi(\eta)=1 \text{ at } \eta=0 \\ f(\eta)=0, f'(\eta)=0, \theta(\eta)=0, \phi(\eta)=0 \text{ at } \eta=1 \end{array}\right\} \tag{9}$$

where

$$R=\frac{ah^2}{\nu}, M=\frac{\sigma B_0^2 h^2}{\rho\nu}, \mathrm{Pr}=\frac{\mu}{\rho_f\alpha}, Sc=\frac{\mu}{\rho_f D}$$

$$Kc=\frac{k_0}{a}, \lambda=\frac{Qh^2}{\mu C_p}, \frac{1}{K_p}=\frac{h^2}{\rho k_p} \tag{10}$$

The physical quantities of interest such as rate of shear stress via skin friction coefficient, rate of heat and mass transfer coefficients via Nusselt number and Sherwood number are given by

$$C_f=f''(0), Nu=-\theta'(0), Sh=-\phi'(0).$$

III. RESULTS AND DISCUSSION

The nanofluid flow between parallel plates through porous media has been studied in the present paper. The effects of heat source/sink and the chemical reaction are also taken care of in the present investigation by incorporating these phenomena in the heat transfer and solutal concentration equation. The main attraction of the paper is the study of thermophoresis and Brownian motion parameters affecting the nanofluid velocity, temperature, and concentration. The transformed governing ordinary differential equations are converted into a set of first-order differential equations with initial conditions and these are solved numerically using Runge-Kutta fourth-order method associated with shooting technique. First of all the higher-order differential equations are discretized into a set of first-order ODEs. Due to a lack of initial conditions, we assume the unknown values for $f''(0)$, $\theta'(0)$ and $\phi'(0)$. These unknowns are obtained by using the Nachtsheim-Swigert shooting iteration technique and

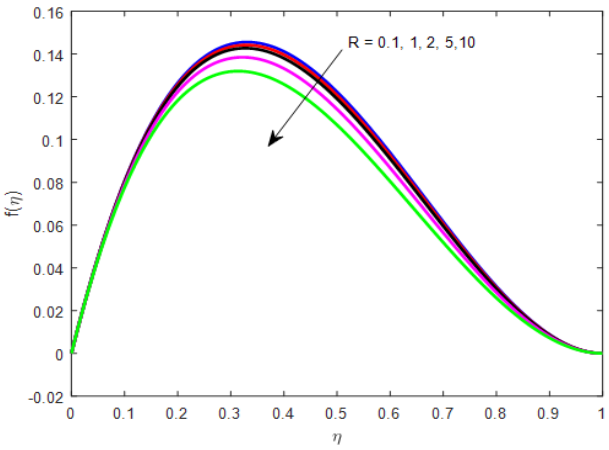

Fig. 2: Influence of velocity ratio parameter on velocity profile for $M = 1$, $Kp = 100$, $Pr = 10$, $Nb = 0.1$, $Nt = 0.1$, $\lambda = 0$.

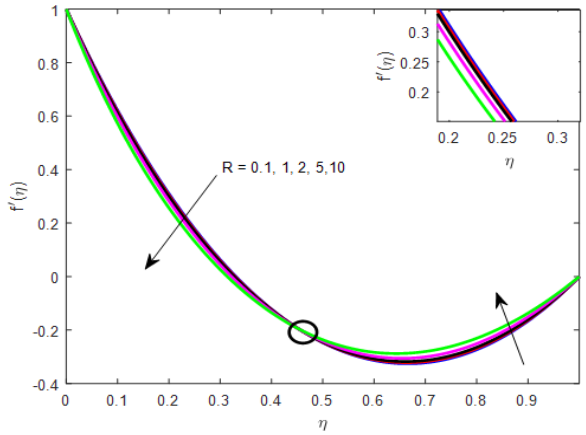

Fig. 3: Influence of velocity ratio parameter on the longitudinal velocity profile for $M = 1$, $Kp = 100$, $Pr = 10$, $Nb = 0.1$, $Nt = 0.1$, $\lambda = 0$.

with proper values of the initial condition, the set of ODEs is solved by employing the Runge-Kutta fourth-order method. The effect of physical parameters characterizes the flow phenomena are obtained and presented in figures. The validation of the present result with the results of Sheikholeslami *et al*. (2016) in the absence of porous matrix Kp ($Kp = 100$), heat source/sink λ ($\lambda = 0$), and chemical reaction parameter Kc ($Kc = 0$), and it is found to be in good agreement. Figures 2 and 3 exhibit the effect of the velocity ratio parameter on transverse and longitudinal velocity profiles respectively in the absence of porous matrix Kp ($Kp = 100$). From Fig. 2 it is observed that the velocity increases near the plate and there is a peak about the region $\eta = 0.3$ and afterward it decreases to meet the boundary condition whereas an increase in velocity ratio parameter the profile decreases significantly. This is because an increase in kinematic viscosity decreases the velocity ratio parameter resulted in decreases in the velocity profile. In the absence of porous matrix Kp ($Kp = 100$) present result well agrees with the result of Sheikholeslami *et al.* (2016). From Fig. 3 it is clear to remark that the longitudinal velocity profile decreases up to the region $\eta < 0.7$ and then increases.

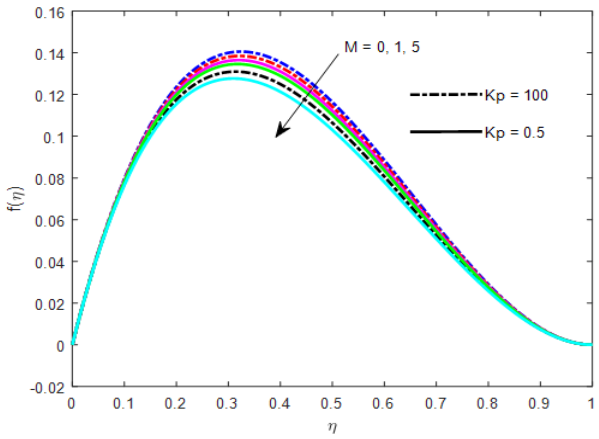

Fig. 4: Influence of magnetic parameter and porous matrix on velocity profile for $R = 5$, $Pr = 10$, $Nb = 0.1$, $Nt = 0.1$, $\lambda = 0$, $Sc = 0.1$, $Kc = 0$.

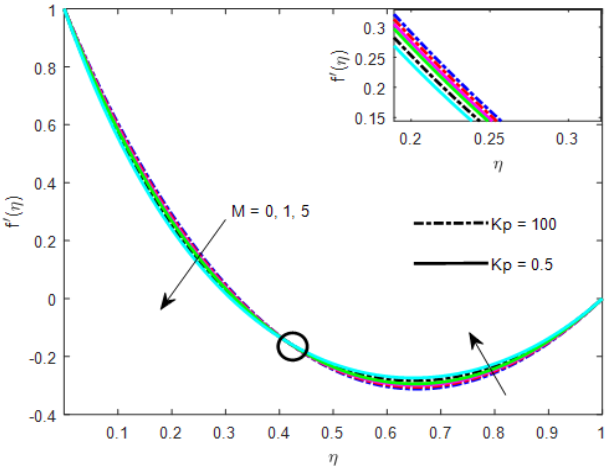

Fig. 5: Influence of magnetic parameter and porous matrix on longitudinal velocity profile for for $R = 5$, $Pr = 10$, $Nb = 0.1$, $Nt = 0.1$, $\lambda = 0$, $Sc = 0.1$, $Kc = 0$.

But dual character is observed for various values of viscosity ratio parameter i.e. for increasing values of ratio parameter longitudinal velocity decreases up to a region $\eta < 0.45$ then increase with a reverse effect to meet the desired boundary condition. Influence of M in the absence porous matrix Kp ($Kp = 100$) and the presence of porous matrix Kp ($Kp = 0.5$) on the transverse and longitudinal velocity profiles respectively are shown in Figs. 4 and 5. In the absence of a magnetic parameter $M = 0$ and porous matrix ($Kp = 100$), our result coincides with the results of Sheikholeslami *et al.* (2016). Also, when $M = 1$ and $Kp = 100$ it validates with the results Sheikholeslami *et al.* (2016). From Fig. 4 it is clear to remark that an increase in magnetic parameter decelerates the transverse velocity profile of the nanofluid. It is because the interaction of the magnetic parameter produces Lorentz force which is an electromotive force that tends to lower down the velocity profile. A peak in nanofluid velocity occurs due to the absence of magnetic field strength. In Fig. 5, the longitudinal velocity also decreases within a region and then after the trend becomes reversed. The presence of a porous matrix retards both the velocity profiles as well.

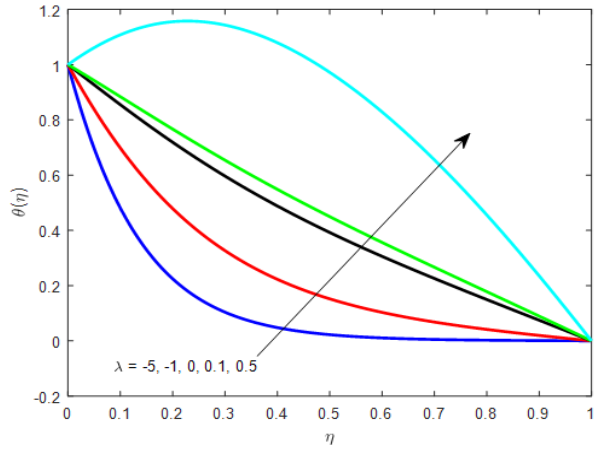

Fig. 6: Influence of velocity ratio parameter on a temperature profile for $R = 5$, $M = 1$, $Kp = 0.5$, $\Pr = 10$, $Nb = 0.1$, $Nt = 0.1$, $Sc = 0.1$, $Kc = 0$.

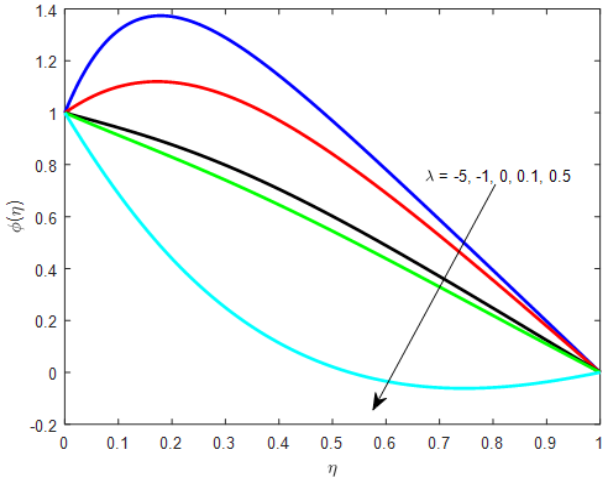

Fig. 7: Influence of velocity ratio parameter on concentration profile for $R = 5$, $M = 1$, $Kp = 0.5$, $\Pr = 10$, $Nb = 0.1$, $Nt = 0.1$, $Sc = 0.1$, $Kc = 0$.

Figures 6 and 7 show the effect of heat source/sink in the presence of a porous matrix on the temperature and concentration profiles for various values of other pertinent physical parameters. The absence of heat source/ sink well agrees with the work of Sheikholeslami *et al*. (2016). From the Fig.6, the increase in heat source enhances the nanofluid temperature significantly. However, the reverse effect is encountered in the presence of heat sink i.e. heat sink retards the nanofluid temperature at all the points in the thermal boundary layer. Moreover, from Fig. 7 it is clear to observe that, due to thermophoresis and Brownian motion parameters the temperature and concentration equations are coupled and solutal concentration also affected by the heat source/sink parameter. Concentration profile retards due to an increase in heat source whereas sink enhances it in the concentration boundary layer.

The effect of the Brownian motion parameter on temperature and concentration is shown in Figs. 8 and 9 for fixed values of involved parameters in the flow phenomena. Heat energy is enhanced by increasing the value of the Brownian parameter whereas retardation in solutal concentration is marked significantly. A similar observation is marked for the variation in the thermophoresis parameter on temperature and concentration profiles (Figs. 10 and 11). Figure12 presents the behavior of generative chemical reaction ($Kc < 0$), no chemical reaction ($Kc = 0$), and destructive chemical reaction ($Kc > 0$) in the presence of porous matrix and other fixed values of physical parameters on the temperature profiles. It is observed that destructive chemical reaction diffuses the solutal

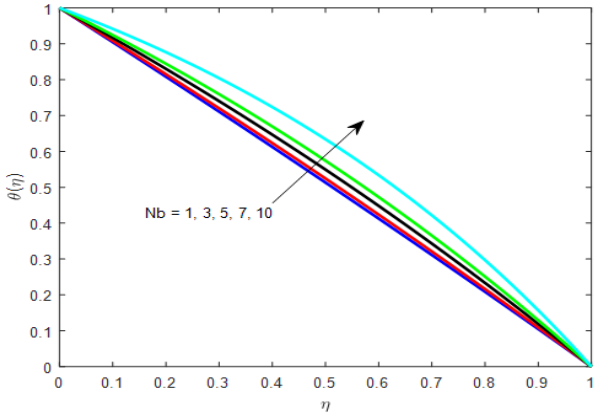

Fig. 8: Influence of Brownian motion parameter on a temperature profile for $R = 5$, $M = 1$, $Kp = 0.5$, $\Pr = 10$, $Nt = 0.1$, $Sc = 0.1$, $Kc = 0$.

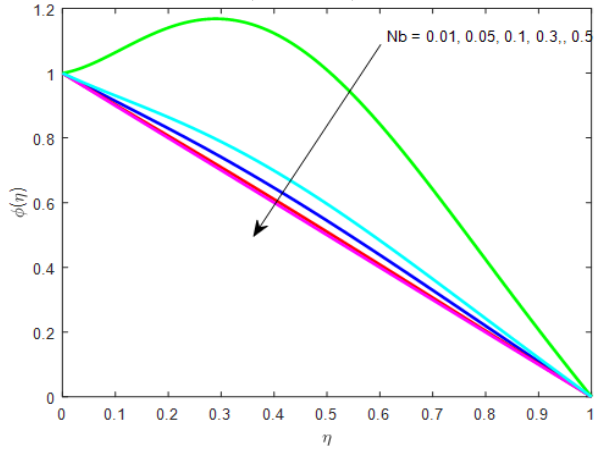

Fig. 9: Influence of Brownian motion parameter on concentration profile for $R = 5$, $M = 1$, $Kp = 0.5$, $\Pr = 10$, $Nt = 0.1$, $Sc = 0.1$, $Kc = 0$.

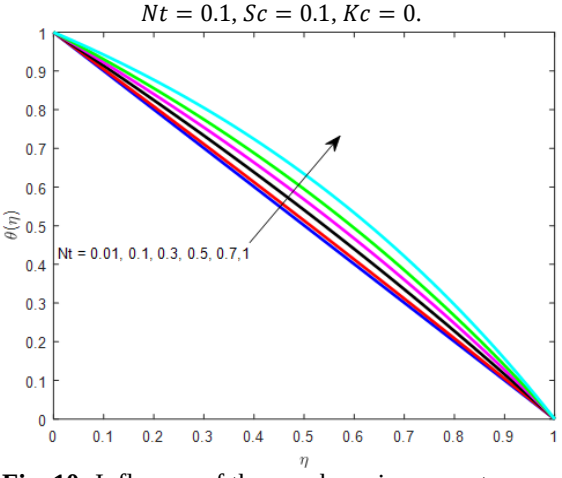

Fig. 10: Influence of thermophoresis parameter on a temperature profile for $R = 5$, $M = 1$, $Kp = 0.5$, $\Pr = 10$, $Nb = 0.1$, $Sc = 0.1$, $Kc = 0$.

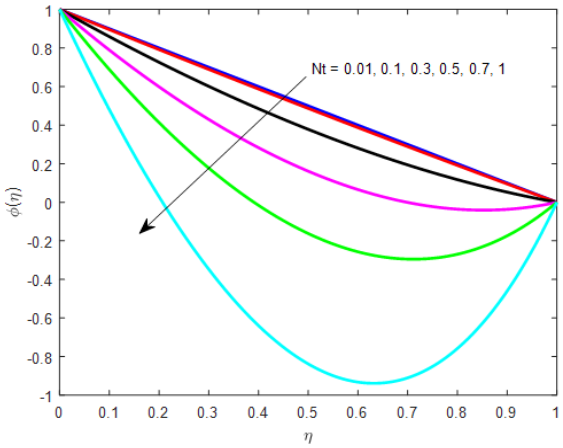

Fig. 11: Influence of thermophoresis parameter on concentration profile for $R = 5$, $M = 1$, $Kp = 0.5$, Pr $= 10$, $Nb = 0.1$, $Sc = 0.1$, $Kc = 0$.

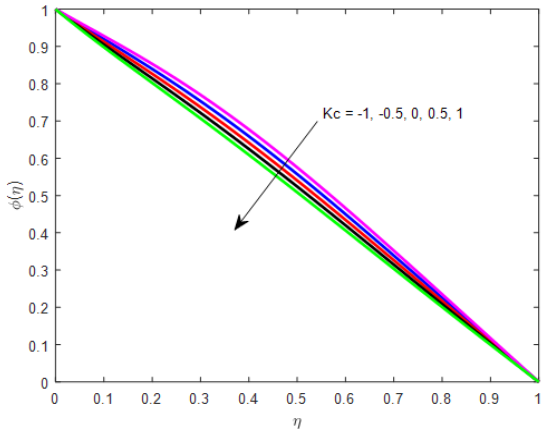

Fig. 12: Influence of chemical reaction parameter on a temperature profile for $R = 5$, $M = 1$, $Kp = 0.5$, Pr $= 10$, $Nb = 0.1$, $Sc = 0.1$, $Nt = 0.1$.

Table1. Skin friction coefficient, Nusselt number for the various thermophysical parameters.

R	M	Kp	Nb	Nt	λ	Sc	Kc	$f''(0)$	$-\theta'(0)$	$-\phi'(0)$
1	1	100	0.1	0.1	0	0.1	0	4.21706994	1.48043451	0.52378508
2								4.30087921	1.4747454	0.53363629
3								4.38432415	1.46916504	0.54332241
1	2							4.34404422	1.47229656	0.53187112
	3							4.46799261	1.46450531	0.53961248
	1	0.1						5.36767833	1.41233712	0.59144281
		0.5						4.46676759	1.46458160	0.53953660
			0.1						1.46458161	0.53953669
			0.2						1.45840328	0.77523616
			0.3						1.45223890	0.85379791
			0.1	0.1					1.46458161	0.53953669
				0.2					1.39147292	0.22068979
				0.3					1.32376951	0.03200713
				0.1	-0.5				2.65129053	-0.64793431
					0				1.46458161	0.53953669
					0.5				-1.3439770	3.35140445
						0.1			-1.3439771	3.35140441
						0.22			-1.3439323	3.36028912
						0.6			-1.3437893	3.38854323
						0.1	-0.5		-1.3440031	3.34301621
							0		-1.3439770	3.35140453
							0.5		-1.3439503	3.35976144

concentration resulted in a decrease in the thermal boundary layer as well as the nanofluid temperature. However, generative chemical reaction enhances the concentration of the nanofluid in the solutal boundary layer.

Finally, the numerical computation of physical quantities for various pertinent parameters characterizing the flow phenomena is obtained and presented in Table 1.

Validation of the present result with the established results of Sheikholeslami *et al*. (2016) is obtained and found to be in good agreement. Further, from Table 1 it is clear to observe that rate of shear stress and rate of mass transfer viz Sherwood number increase with an increase in viscosity parameter however, the rate of heat transfer via Nusselt number decreases. Also, it is interesting to note that the higher density in the porous medium in the nanofluid increases the skin friction coefficient, and the rate of heat transfer decreases. This suggests that the presence of a porous matrix can be treated as the coolant in nanofluid for the production processes of material in manufacturing industries. An increase in the Brownian motion parameter and thermophoresis parameter retards the heat transfer rate as well but the effects of these parameters on mass transfer rate are diversified from each other. It is clear to remark that Brownian motion is favorable to enhance the rate of mass transfer whereas thermophoresis decreases it. The effect of heat source/sink is also crucial in the rate of heat and mass transfer. It is seen that the heat transfer rate gets enhanced with an increase in source further, the reverse effect is observed in the case of the sink. Finally, heavier species is favorable to increase the mass transfer rate but with an inclusion of destructive chemical reactant further, constructive chemical reaction parameter decreases it significantly.

IV. CONCLUSION

Two-dimensional, electrically conducting nanofluid flow past in between two horizontal plates through a porous

medium is considered in the present study. Analytical approach to the nonlinear coupled ODEs does not hold good therefore, these are solved numerically with the help of the Runge-Kutta fourth-order method. Influence of embedding physical parameter on the flow phenomena are obtained and discussed. Numerical computations of various physical quantities are also obtained for different characterizing parameters and presented in the table and further discussed elaborately. The main findings of the aforesaid results are as follows:

- The convergence procedure of the mathematical method used at present is well confirmed with earlier established results.
- Decay in the velocity boundary layer is marked due to an increase in velocity ratio parameter whereas the longitudinal velocity profile shows a dual character.
- The longitudinal velocity profile fails to enhance due to the presence of a porous matrix.
- The thickness of the thermal boundary layer becomes thinner and thinner due to the presence of sink however, the source enhances it.
- The sink is favorable to increase the rate of heat transfer but the source fails.
- Heavier species is useful to enhance the rate of mass transfer whereas the generative chemical reaction parameter decreases it.

REFERENCES

Baag, S., Mishra, S.R., Dash, G.C. and Acharya, M.R. (2017) Numerical investigation on MHD micropolar fluid flow toward a stagnation point on a vertical surface with the heat source and chemical reaction. *Journal of King Saud Engineering Sciences*. **29**, 75-83.

Bhattacharyya, K., Hayat, T. and Alsaedi, A. (2013) Analytic solution for magnetohydrodynamic boundary layer flow of Casson fluid over a stretching/shrinking sheet with wall mass transfer. *Chin. Phys. B.*, **22**, 0247021–0247026.

Bhukta, D., Dash, G.C. and Mishra, S.R. (2014) Heat and Mass Transfer on MHD Flow of a Viscoelastic Fluid through Porous Media over a Shrinking Sheet. *International Scholarly Research Notices*, **2014**, 572162.

Choi, S. (1995) Enhancing thermal conductivity of fluids with nanoparticles. *ASME-Publ. Fed*. **231**, 99–106.

Gangadhar, K., Ramana, K.V., Ibrahim, S.M. and Makinde, O.D. (1028a) Slip flow of an unsteady nanofluid past a stretching surface in a transverse magnetic field using SRM. *Defect and Diffusion Forum*. **387,** 562–574.

Gangadhar, K., Babu, P.R.S. and Makinde, O.D. (2018b) Spectral relaxation method for Powell-Eyring fluid flow past a radially stretching heated disk surface in a porous medium. *Defect and Diffusion Forum*, **387**, 575–586.

Gireesha, B.J., Archana, M., Prasanna Kumara, B.C., Gorla, R. and Makinde, O.D. (2017) MHD three dimensional double-diffusive flow of Casson nanofluid with buoyancy forces and nonlinear thermal radiation over a stretching surface. *International Journal of Numerical Methods for Heat and Fluid Flow*. **27**, 2858-2878.

Ibrahim, W. and Makinde, O.D. (2016) Magnetohydrodynamic stagnation point flow and heat transfer of Casson nanofluid past a stretching sheet with slip and convective boundary condition. *Journal of Aerospace Engineering*. **29**, 04015037.

Kar, M., Dash, G.C. and Rath, P.K. (2013) Three dimensional free convective MHD free flow on a vertical channel through a porous medium with the heat source and chemical reaction. *J. Engg. Thermo physics*, **22**, 203-215.

Khan, W.A., Makinde, O.D. and Khan, Z.H. (2016) Non-aligned MHD stagnation point flow of variable viscosity nanofluids past a stretching sheet with radiative heat. *International Journal of Heat and Mass Transfer*. **96**, 525-534.

Lai, E.C. and Kulacki, F.A. (1990) Effects of variable viscosity on convective heat transfer along a vertical surface in a saturated porous medium. *Int. J. Heat Mass Transfer*. **33,** 1028-1031.

Mahanthesh, B., Gireesha, B.J., Gorla, R.S.R. and Makinde, O.D. (2018) Magnetohydrodynamic three-dimensional flow of nanofluids with slip and thermal radiation over a nonlinearly stretching sheet: a numerical study. *Neural Computing and Applications*, **30**, 1557–1567.

Makinde, O.D., Das, S. and Jana, R.N. (2016a) Effects of Navier slip on MHD chemically reacting nanofluid over a convective permeable surface with radiative heat. *Journal of Nanofluids*, **5**, 687-695.

Makinde, O.D., Khan, W.A. and Khan, Z.H. (2016b) Analysis of MHD nanofluid flow over a convectively heated permeable vertical plate embedded in a porous medium. *Journal of Nanofluids,* **5**, 574-580.

Makinde, O.D., Khan, W.A. and Khan, Z.H. (2017) Stagnation point flow of MHD chemically reacting nanofluid over a stretching convective surface with slip and radiative heat. *Proceedings of the Institution of Mechanical Engineers, Part E: Journal of Process Mechanical Engineering.* **231**, 695–703.

Nadeem, S., Haq, R.U. and Lee, C. (2012) MHD flow of a Casson fluid over an exponentially shrinking sheet. *Sci. Iranic.*, **19,** 1550–1553.

Nadeem, S., Haq, R.U., Akbar, N.S., Lee, C. and Khan, Z.H. (2013) Numerical study of boundary layer flow and heat transfer of Oldroyd-B nanofluid towards a stretching sheet. *PLOS One*. **8**, 1-6.

Prasad, K.V., Vajravelu, K., Vaidya, H. and Van Gorder, R.A. (2017) MHD Flow and Heat Transfer in a Nanofluid over a Slender Elastic Sheet with Variable Thickness. *Results in Physics.* **7**, 1462-1474.

Prasad, K.V., Vaidya, H., Makinde, O.D. and Setty, B.S. (2019) MHD Mixed Convective Flow of Casson Nanofluid over a Slender Rotating Disk with

Source/Sink and Partial Slip Effects. *Defect and Diffusion Forum*, **392**, 92-122.

Seikholeslami, M., Rashidi, M.M., Alsaad, M.M., Firouzi, F., Rokni, H.B. and Domairry, G. (2016) Steady nanofluid flow between parallel plates considering thermophoresis and Brownian effects. *Journal of King Saud University*. **28**, 380-389.

Sharma, R.P., Choudhary, S. and Makinde, O.D. (2017a) MHD Slip flow and heat transfer over an exponentially stretching permeable sheet embedded in a porous medium with the heat source. *Frontiers in Heat and Mass Transfer*, **9**, 013018.

Sharma, R.P., Avinash, K., Sandeep, N. and Makinde, O.D. (2017b) Thermal radiation effect on non-Newtonian fluid flow over a stretched sheet of non-uniform thickness. *Defect and Diffusion Forum*, **377,** 242-259.

Vajravelu, K., Prasad, K.V., Ng, C.-O., and Vaidya, H. (2017) MHD squeeze flow and heat transfer of a nanofluid between parallel disks with variable fluid properties and transpiration. *International Journal of Mechanical and Materials Engineering*, **12**, 9.

Received: October 30, 2019
Sent to Subject Editor February 21, 2020
Accepted July 26, 2020
Recommended by Subject Editor Gianfranco Caruso